Posttranslational modification and proteolytic processing of urinary osteopontin

Brian Christensen, Torben E. Petersen, Esben S. Sørensen, Esben S. Sørensen

Posttranslational modification and proteolytic processing of urinary osteopontin

Brian Christensen, Torben E. Petersen, and Esben S. Sørensen‡

Protein Chemistry Laboratory, Department of Molecular Biology and Interdisciplinary Nanoscience Center (iNANO), University of Aarhus, Gustav Wieds Vej 10C, DK-8000 Aarhus C, Denmark

‡Corresponding author: Esben S. Sørensen, Protein Chemistry Laboratory, Department of Molecular Biology, University of Aarhus, Gustav Wieds Vej 10C, DK-8000 Aarhus C, Denmark. Tel.: 45 89425092; Fax: 45 89425044; E-mail: ess@mb.au.dk

Keywords: Osteopontin, phosphorylation, sulphation, O-glycosylation, uropontin

Abbreviations used: OPN, osteopontin; PTM, posttranslational modification; RGD, Arg-Gly-Asp; COM, calcium oxalate monohydrate; COD, calcium oxalate dihydrate; ALP, bovine alkaline phosphatase; µRPC, µ reverse-phase chromatography; PNGase F, Peptide-N-Glycosidase F; RP, reverse-phase; TFA, trifluoroacetic acid; MALDI-TOF-MS, matrix-assisted laser desorption ionization time-of-flight mass spectrometry; GalNAc, N-acetylgalactosamine; GlcNAc, N-acetylglucosamine; Sia, sialic acid; PTH, phenylthiohydantoin; MMP, metalloproteinase.

Short title: Modification and proteolytic processing of OPN

Abstract

Osteopontin (OPN) is a highly phosphorylated glycoprotein present in many tissues and body fluids. In urine OPN is a potent inhibitor of nucleation, growth and aggregation of calcium oxalate crystals suggesting a role in the prevention of renal stone formation. The role of OPN in nephrolithiasis is however somewhat unclear as it may also be involved in urinary stone formation, and it has been identified among the major protein components of renal calculi. Most likely the function of OPN in urine is dependent upon the highly anionic character of the protein. Besides a very high content of aspartic- and glutamic acid residues, OPN is subjected to significant posttranslational modification (PTM), such as phosphorylation, sulphation and glycosylation, which may function as regulatory switches in promotion or inhibition of mineralization. In the present study we have characterized the PTMs of intact human urinary OPN and N-terminal fragments thereof. Mass spectrometric (MS) analysis showed a mass of 37.7 kDa for the intact protein. Enzymatic dephosphorylation and peptide mass analyses demonstrated that the protein contains approximately eight phosphate groups distributed over 30 potential phosphorylation sites. In addition one sulphated tyrosine and five O-linked glycosylations were identified in OPN, whereas no N-linked glycans were detected. Peptide mapping and immunoblotting using different monoclonal antibodies showed that the N-terminal fragments present in urine are generated by proteolytic cleavage at Arg^{228}-Leu^{229} and Tyr^{230}-Lys^{231}.

Introduction

Osteopontin (OPN) is a phosphorylated glycoprotein containing an integrin binding RGD (Arg-Glu-Asp) sequence. The protein was originally purified from the mineralized matrix of bovine bone [1], however, the expression of OPN is not limited to mineralized tissues but extends to most tissues and body fluids including milk, blood and urine [2]. OPN consists of approximately 300 amino acid residues with a very high content of aspartic- and glutamic acid. The protein is involved in a broad range of functions in both physiological and pathological processes like cytokine production, tumor growth, inflammation and mineralization [3-5]. Furthermore, OPN is a key molecule in bone remodelling [5, 6] and it hinders ectopic calcification by inhibiting the formation of hydroxyapatite [7, 8], which is the main mineral phase of bone and teeth,

as well as calcium oxalate [9], the main mineral in renal calculi.

OPN is found at high levels in urine with an average of approximately four mg secreted into human urine daily [10]. In contrast, OPN is undetectable in normal kidney tissues [11], indicating that the OPN produced in the renal tubules is immediately secreted in the urine. OPN can inhibit nucleation, growth and aggregation of calcium oxalate crystals *in vitro* [9, 12, 13], and it blocks binding of the crystals to renal epithelial cells [14]. In addition, calcium oxalate monohydrate (COM) crystal growth and aggregation are inhibited by 50% at an OPN concentration between 16 to 28 nM, a concentration that is an order of magnitude lower than the OPN concentration of 131 nM found in normal urine [13]. OPN also favours the formation of calcium oxalate dihydrate (COD) over COM crystals [12]. The induction of COD by OPN may be protective against calcium oxalate nephrolithiasis since COD has demonstrated less affinity for attachment to renal epithelial cells than COM [12]. Besides reducing crystal affinity for renal cells, OPN may act as an intracrystalline protein assisting stone prevention by rendering crystals more susceptible to intracellular degradation [15]. Furthermore, OPN knockout mice fed an crystal-inducing diet developed renal calcium oxalate stones while wild type mice were completely unaffected, perhaps due to an up-regulated OPN expression in response to the induced hyperoxaluria suggesting a protective role of OPN [16]. Similarly, a recent study showed that 10% of mice lacking OPN spontaneously formed renal stones and 65% developed renal crystals under experimentally induced hyperoxaluria, whereas these events were not observed in wild type mice [17].

There are many indications that OPN is an important inhibitor of renal stone formation, however, the protein has also been implicated as a promoter of stone formation. One study showed increased calcium oxalate crystal adherence to kidney cells when they were incubated with OPN [18]. Furthermore, inhibition of OPN synthesis has been shown to suppress the deposition and adhesion of calcium oxalate crystals to rat renal cells [19], and addition of polyclonal OPN antibodies reduced the deposition of crystals on the surface of kidney cells [20]. It has also been suggested that OPN is involved in urinary stone formation [21], and the protein has been identified as a prominent constituent of the major matrix of renal calculi [22]. Reduced OPN levels in stone formers compared to non-stone formers have been reported in one study [23], while no difference in urinary OPN levels has been reported in other studies [24, 25].

OPN is extensively altered through posttranslational modification (PTM), such as phosphorylation, sulphation, glycosylation and proteolytic processing, which have significant implications on the structure and the biological function of the protein [26]. The PTMs of OPN from bovine and human milk as well as rat bone have been thoroughly characterized [27-29]. Recently, a comparative study of OPN produced by murine *ras*-transformed fibroblasts and differentiating osteoblasts demonstrated remarkably different phosphorylation patterns between OPNs originating from the same species, which translated into significant functional differences in cellular adhesion [30].

The PTMs of OPN provide a basis for its regulatory functions in mineralization processes, as dephosphorylated OPN has been shown to loose the ability to inhibit hydroxyapatite formation [7, 8]. Emphasizing the importance of the phosphorylations, it was recently shown that highly phosphorylated milk OPN promoted hydroxyapatite formation and growth, whereas the less phosphorylated bone OPN inhibited these processes [31]. Similarly, recombinant (non-phosphorylated) OPN increases mineralization of vascular smooth muscle cells, whereas enzymatically phosphorylated OPN is a potent inhibitor of this process [32]. Recently, it was shown that only phosphorylated OPN dose-dependently inhibited mineralization of MC3T3-E1 osteoblast cell cultures [33]. Phosphorylation of OPN peptides also markedly enhanced the inhibition of hydroxyapatite and COM crystal growth [34, 35] and C-terminal fragments of urinary OPN can inhibit COM growth as efficient as the intact protein, suggesting that different parts of the protein can regulate crystal formation [36].

Western blotting of human urinary OPN has shown the presence of different forms in the 40-70 kDa range [15, 24, 25]. The structural variation underlying these differences in migration is unknown. Normal rat kidney cells have been shown to produce both phosphorylated and non-phosphorylated OPN which also diverge in glycosylation and physiological properties [37]. Furthermore, low molecular weight OPN variants probably resulting from cleavage by serine proteases are present at a higher frequency in urine from individuals with kidney stone disease than in urine from healthy individuals [24]. Recently, a series of C-terminal OPN fragments were identified by two-dimensional electrophoresis and mass spectrometry in patients with ovarian cancer, but not in healthy controls [38]. In the present study we have separated and characterized different forms of human urinary OPN with regard to PTMs and

proteolytic processing. These modifications are likely to be key factors in the regulatory roles of OPN in renal stone formation.

Experimental

Materials

The monoclonal mouse antibodies 1H3 and 3D9 [39] were a kind gift from Dr. David T. Denhardt, Rutgers University, NJ. Swine anti-rabbit and rabbit anti-mouse immunoglobulins conjugated to alkaline phosphatase were from DAKO (Glostrup, Denmark). Bovine pancreas trypsin and *Staphylococcus aureus* V8 proteinase were obtained from Worthington Biochemical (Freehold, NJ). Thermolysin, bovine alkaline phosphatase (ALP), human plasma thrombin and arylsulphatase were from Sigma (St. Louis, MO). The μRPC (μ reverse-phase chromatography) C_2/C_{18} PC 2.1/10 column, Protein A sepharose CL-4B resin, DEAE sepharose material and PD-10 desalting columns were from GE Healthcare (Uppsala, Sweden). Vydac C_4 and C_{18} RP (reverse-phase) resin were obtained from The Separations Group (Hesperia, CA). Reagents used for sequencing were purchased from Applied Biosystems (Warrington, UK). 2,5-dihydroxybenzoic acid was from LaserBio Labs (Sophia-Antipolis Cedex, France). The Peptide-N-Glycosidase F (PNGase F) kit was obtained from New England Biolabs (Beverly, MA). All other chemicals used were of analytical grade.

Polyclonal OPN Antibodies

Polyclonal antiserum against human milk OPN was raised in rabbits at DAKO (Glostrup, Denmark). OPN specific polyclonal antibodies were isolated from the rabbit serum on a Protein A sepharose column. The specificity of the antibodies was checked and verified by Western blot analyses of milk samples and purified OPN.

Western Blotting

OPN (50 ng/lane) and urine (10 uL) were loaded onto 16% tris-tricine gels, fractionated by SDS-PAGE and electrophoretically transferred to Hybond-P polyvinylidene difluoride membranes (GE Healthcare) for immunodetection. The membranes were blocked in 2% tween in tris-buffered-saline before addition of either polyclonal rabbit OPN antibodies (5 μg/ml) or monoclonal mouse OPN antibodies 1H3 and 3D9 (1.5 μg/ml). OPN was detected with alkaline phosphatase conjugated secondary

immunoglobulins.

Purification of OPN

Urine samples were collected from seven healthy donors with normal renal function and no history of urinary disease and frozen at -80 °C. Thawed urine samples were centrifuged at 4500 *g* for 30 minutes and the resulting supernatant was incubated with DEAE sepharose material at pH 8.1 for 2 h at room temperature. Adsorbed proteins were batch eluted with stepwise increasing concentrations of ammonium bicarbonate (pH 8.1). The batch containing OPN was lyophilized, followed by passage through a PD10 column in 20% formic acid. The salt free eluate was lyophilized and subjected to further purification by RP-HPLC on a Vydac C_4 column connected to a GE Healthcare LKB system. Separation was carried out at 40 °C in 0.1% trifluoroacetic acid (TFA) (buffer A) and eluted with a gradient of 80% acetonitrile in 0.1% TFA (buffer B) developed over 50 min (0-5 min, 0% B; 5-40 min, 0-50% B; 40-50 min, 50-95% B) at a flow rate of 0.85 ml/min. The peptides were detected in the effluent by measuring the absorbance at 226 nm. The fraction containing OPN was identified by immunodetection and N-terminal sequencing. The full-length protein (OPN60) and N-terminal fragments (OPN45 and OPN50) were separated by RP-HPLC on a Vydac C_{18} column and eluted with stepwise increasing concentrations between 10% and 30% of 75% 2-propanol in 0.1% TFA. The fractions were analyzed by N-terminal sequencing and SDS-PAGE, and proteins were visualized by Coomassie staining or by Western blotting. The amount of purified OPN was determined by amino acid analysis.

Phosphate content of OPN

Native and dephosphorylated OPN isoforms were analyzed by MS using a Voyager DE-PRO MALDI-TOF (matrix-assisted laser desorption ionization time-of-flight) mass spectrometer (Applied Biosystems). Samples for MS analyses were prepared by mixing the sample with a saturated solution of 2,5-dihydroxybenzoic acid in a 1:1 ratio directly on the MS-target probe. All spectra were obtained in positive linear-ion mode using a nitrogen laser at 337 nm and an acceleration voltage of 20 kV. Typically, 50-100 laser shots were added per spectrum and calibrated with external standards. The masses were assigned using the half-height width method. For dephosphorylation, 2.5 µg OPN was incubated with 0.07 U ALP in 10 mM ammonium bicarbonate (pH 8.5) overnight at 37

°C. The average phosphate content estimated by MS was confirmed with a phosphoprotein phosphate estimation assay kit (Pierce, Rockford, IL).

Carbohydrate analyses

Full-length OPN (OPN60) was quantified by amino acid analysis and hydrolyzed in 2 M TFA for 4 h at 100 °C under oxygen-free conditions. α-L-rhamnose was added as internal standard. For quantification of the more stable amino sugars, N-acetylgalactosamine (GalNAc) and N-acetylglucosamine (GlcNAc), an additional OPN sample was hydrolyzed in 4 M HCl for 6 h at 110 °C. For sialic acid (Sia) analysis, the protein was hydrolyzed in 0.1 M HCl for 60 min at 80 °C. Monosaccharides were separated by high-pH anion-exchange chromatography using a CarboPac PA1 column (4 x 250 mm) (Dionex, Sunnyvale, CA) and monitored by pulsed electrochemical detection. The neutral monosaccharides were eluted isocratically with 16 mM NaOH, whereas Sia was eluted with 100 mM NaOH, 150 mM sodium acetate. Standard monosaccharide mixtures of α-L-fucose, D-galactosamine, D-glucosamine, D-galactose, D-glucose (all 0.1 mM), D-mannose (0.5 mM), α-L-rhamnose (0.2 mM) and N-acetylneuraminic acid (0.02 mM) (all from Sigma) were used. Linearity was observed between the injected amounts of monosaccharide standards and the peak areas, and hence the amounts of the individual monosaccharides in the samples were deduced from standard curves.

Removal of potential N-linked glycosylations was performed as described by the manufacturer using a PNGase F deglycosylation kit. OPN was incubated with 500 U PNGase F at 37 °C for 20 h. The reaction products from the enzymatic deglycosylation were analyzed by SDS-PAGE.

Generation and separation of peptides

OPN was digested with trypsin using an enzyme to substrate ratio of 1:30 (w/w) in 0.1 M ammonium bicarbonate at 37 °C for 6 h. Tryptic peptides were separated by RP-HPLC on a μRPC C_2/C_{18} PC 2.1/10 column connected to a GE Healthcare SMART system. Separation was carried out in 0.1% TFA (buffer A) and eluted with a gradient of 60% acetonitrile in 0.1% TFA (buffer B) developed over 54 min (0-9 min, 0% B; 9-49 min, 0-50% B; 49-54 min, 50-100% B) at a flow rate of 0.15 ml/min. The peptides were detected in the effluent by measuring the absorbance at 214 nm. A fragment

(residues Gln^{36}/Ser^{62}-Arg^{143}) from the tryptic digest was further digested with thermolysin in 0.1 M pyridine-acetate (pH 6.5), 5 mM $CaCl_2$ at 56 °C for 6 h. The resulting peptides were separated as described for the tryptic digest. A glycopeptide (residues Leu^{116}-Thr^{139}) from the thermolysin digest was further digested with *S. aureus* V8 proteinase in 0.1 M ammonium bicarbonate (pH 8.1) at 37 °C for 3.5 h.

OPN45/OPN50 and OPN60 were digested with thrombin (0.05 U/µg OPN) in 0.1 M ammonium bicarbonate at 37 °C for 1 h. The generated fragments were separated by RP-HPLC on a Vydac C_{18} column connected to a GE Healthcare LKB system. Separation was carried out in 0.1% TFA (buffer A) and eluted with a gradient of 75% 2-propanol in 0.1% TFA (buffer B) developed over 80 min (0-5 min, 0% B; 5-70 min, 0-50% B; 70-80 min, 50-95% B) at a flow rate of 0.85 ml/min.

Characterization of peptides

Peptides and fragments were characterized by mass spectrometric and amino acid sequence analyses. All MS spectra were obtained in both positive reflector-ion and positive linear-ion mode as described above. The theoretical peptide masses and sequence coverage were calculated using the GPMAW program (Lighthouse Data, Odense, Denmark). Amino acid sequence analyses were performed on an Applied Biosystems PROCISE HT protein sequencer with on-line identification of phenylthiohydantoin (PTH)-derivatives. Glycosylated threonine residues were identified by the lack of a PTH-derivate in the cycles where these amino acids are modified.

Sulphate analysis

Modified peptides containing both potential phosphorylation (serines and threonines) and sulphation (tyrosines) sites were dephosphorylated with ALP as described above and analysed by MALDI-TOF-MS. The peptides Phe^{158}-Lys^{187} and Arg^{160}-Lys^{187} were further treated with 0.5 U arylsulphatase in 0.2 M sodium acetate (pH 5.0) at 37 °C for 2 h and then reanalysed by MS.

RESULTS

Purification of OPN from urine – Urine samples from seven healthy donors, with normal renal function and no history of urinary disease, were analysed by Western blotting to examine the molecular forms of OPN in urine (Fig. 1). Urinary OPN was detected with variable intensity in all individuals by a polyclonal antibody. The observed OPN patterns show that all analyzed urine samples contain OPN forms of relative homogenous molecular weight in the range of 45-60 kDa. No, low molecular weight OPN forms were observed in any of the tested individuals.

OPN was purified from human urine by anion-exchange followed by RP-HPLC separation on a Vydac C_4 column (Fig. 2). Sequencing of the OPN containing fraction showed two sequences: a major, $I^{1}PVKQA^{6}$, and a minor, $V^{3}KQADS^{8}$, both corresponding to the N-terminal part of human OPN. SDS-PAGE revealed the presence of three bands migrating at approximately 45 kDa, 50 kDa and 60 kDa, respectively and Western blotting confirmed their OPN nature (Fig. 3A, Lane 1 and 2). In the following these components will be referred to as OPN45, OPN50 and OPN60.

To separate the different forms, the OPNs were subjected to RP-HPLC on a Vydac C_{18} column and eluted with stepwise increasing concentrations of 2-propanol. The elution profile revealed two fractions (insert in Fig. 2). As judged by SDS-PAGE the first fraction contained OPN45 and OPN50 and the second fraction contained OPN60 (Fig. 3A, lane 3 and 4). The monoclonal antibody 1H3 (epitope: S^{218}AETHSH^{224} [39]) recognized all three OPN forms (Fig. 3B, lane 1 and 2), whereas Western blotting with the monoclonal 3D9 (epitope: K^{283}FRISHELDSASSEVN^{298} [39]) showed that only OPN60 contains the extreme C-terminal part of OPN (Fig. 3B, lane 3 and 4). This indicates that OPN60 represents the full-length OPN molecule from human urine, since it contains both the N- and C-terminal, whereas OPN45 and OPN50 are truncated or cleaved forms lacking a C-terminal part of the protein.

Identification of cleavage sites in OPN – To identify the C-terminus and thereby the exact cleavage site that generates OPN45 and OPN50, these proteins were subjected to thrombin cleavage. Reverse-phase separation of the products from the thrombin digest followed by sequence and MS analysis showed the presence of two N-terminal fragments, Ile^{1}-Arg^{152} and Val^{3}-Arg^{152}, and two C-terminal fragments, Ser^{153}-Arg^{228} and Ser^{153}-Tyr^{230} (Table 1). This indicates that OPN45 and OPN50 are generated by cleavage at Arg^{228}-Leu^{229} and/or Tyr^{230}-Lys^{231} in human urine. In an additional

experiment digests of OPN45/OPN50 and OPN60 were compared by peptide mapping analysis. Peptides from the N-terminal part (Ile^{1}-Leu^{229}/Arg^{232}) were found in all OPN isoforms, whereas peptides from the C-terminal part (Leu^{229}-Asn^{298}) only were identified in OPN60, further supporting that OPN45 and OPN50 are generated by cleavage in the region around Leu^{229}-Arg^{232}.

To test whether OPN45/OPN50 could be generated from OPN60 by thrombin cleavage, the full-length protein was incubated with this protease. This resulted in two major fractions in RP-HPLC containing the N-terminal part (Ile^{1}-Arg^{152} and Val^{3}-Arg^{152}) and the expected C-terminal part of OPN (Ser^{153}-Asn^{298}). Furthermore, we observed a minor fraction representing a fragment corresponding to Ser^{153}-Arg^{228}/Tyr^{230}. Judged by RP-HPLC and MS analyses this fraction only represents a very minor portion of the cleavage products and hence we cannot on this basis conclude that thrombin would cleave OPN at this site *in vivo*.

Molecular masses - The masses of the OPNs were determined by linear MALDI-TOF-MS. MS analysis showed a mass of approximately 37.7 kDa for OPN60 (Fig. 4A), whereas the sample containing OPN45 and OPN50 showed one broad mass peak with an average value of approximately 29.3 kDa (Fig. 4B). To estimate the total number of phosphate groups present, OPN60 and the fragments OPN45/OPN50 were treated with ALP. The molecular weight of dephosphorylated OPN60 was 37.1 kDa corresponding to a loss of approximately eight phosphate groups (Fig. 4A). Phosphatase treatment of the N-terminal OPN fragments reduced the mass to 28.8 kDa corresponding to a loss of approximately six phosphorylations (Fig. 4B). This was confirmed by use of a phosphoprotein phosphate estimation kit revealing a total of 7.8 phosphate groups in OPN60 and 6.9 phosphate groups in the sample containing OPN45/OPN50. Subtraction of the theoretical mass of the human OPN polypeptide (33714 Da) from the observed average mass of dephosphorylated OPN60 (37.1 kDa) leaves approximately 3.4 kDa, which must then be accounted for by other PTMs.

Phosphorylations – To identify potential phosphorylation sites in urinary OPN, the OPN fraction (Fig. 2) was digested with trypsin and the resulting peptides were separated by RP-HPLC (data not shown). A large acidic fragment of OPN (Gln^{36}/Ser^{62}-Arg^{143}) not susceptible to tryptic cleavage was further digested with thermolysin and the resulting peptides were separated by RP-HPLC. All fractions from the RP-HPLC separations of peptides were analyzed by MALDI-TOF-MS (Table 2 and

Supplementary Table I and II). In total, the approximately eight phosphate groups in OPN60 were distributed over 30 potential phosphorylation sites. Some of the phosphopeptides contained more serines/threonines than the observed number of phosphorylations. In these cases the phosphate groups were assigned to residues fitting the target sequence of the Golgi kinase/mammary gland casein kinase (S/T-X-E/S(P)/D) based on the localization of phosphorylated residues in other OPN isoforms [27-29]. Data from the peptide phosphorylation analysis are summarized in Table 2 and the resulting map of PTMs is shown in Figure 5, which also contains a comparison with the PTMs of human milk OPN.

Sulphation of OPN – The linear MALDI-TOF-MS spectrum of a peptide covering R^{160}PDIQYPDATDEDITSHMESEELNGAYK^{187} showed *m/z* values of 3307.18, 3387.53, and 3466.42 (Fig. 6A). These masses correspond to Arg^{160}-Lys^{187} with excess masses of ~80 Da, ~160 Da, and ~240 Da, respectively. These masses could correspond to different phosphorylation variants, or they could represent a combination of phosphate and sulphate groups on the peptide. After treatment with ALP an excess mass of ~80 Da remained associated with the peptide (Fig. 6B) strongly indicating that Arg^{160}-Lys^{187} is also sulphated. The presence of a sulphate group was verified by treatment of the dephosphorylated peptide with arylsulphatase which removed the excess mass of 80 Da (Fig. 6C). The peptide Arg^{160}-Lys^{187} contains two potential sites for sulphation (Tyr^{165} and Tyr^{186}). The residue corresponding to Tyr^{165} has been shown to be sulphated in OPN from rat bone [29], and it is therefore most likely that this residue is sulphated in urinary OPN. Two other tyrosine containing peptides, Gln^{5}-Lys^{35} and Gly^{205}-Lys^{225}, were observed with excess masses that could correspond to both phosphorylations and/or sulphate groups (Supplementary Table I). Treatment of these peptides with ALP showed that they only contained phosphate groups. Peptides containing Tyr^{165} in human milk OPN was also analysed for sulphation. However, no indication of this modification was observed in the milk isoform (data not shown).

Glycosylations - All O-glycosylated residues in OPN from urine were located in a single thermolytic peptide, Leu^{116}-Thr^{139}. This peptide was further digested with *S. aureus* V8 proteinase resulting in the two peptides, L^{116}VTDFPTDLPATE^{128} and V^{129}FTPVVPTVDT^{139}, which were separated by RP-HPLC. The peptide L^{116}VTDFPTDLPATE^{128} was observed in linear MS with *m/z* values at 3679.83, 3970.97 and 4261.24 (Table 3). These masses correspond to Leu^{116}-Glu^{128} with three

GalNAc-galactose units and four to six Sia units attached. The lack of a PTH-Thr at the positions of Thr^{118}, Thr^{122} and Thr^{127}, when subjected to Edman sequencing, indicates that these threonines are glycosylated in the peptide. Similarly, MS analysis of the peptide $V^{129}FTPVVPTVDT^{139}$ showed that this peptide contained glycosylations composed of up to two GalNAc, one GlcNAc, two galactose and five sialic acid (Sia) units (Table 3). Edman sequencing showed that Thr^{131} and Thr^{136} are modified. Collectively these data show that Thr^{118}, Thr^{122}, Thr^{127}, Thr^{131} and Thr^{136} are glycosylated in urinary OPN. The absence of any trace of PTH-amino acids in these positions indicates that they are fully glycosylated. The masses of the glycopeptides show that each glycosylated threonine can be modified by different glycan structures, but based on the major mass peaks for both Leu^{116}-Glu^{128} and Val^{129}-Thr^{139} they seem mainly to consist of the disialylated core-1 O-glycan Sia-galactose-[Sia]-GalNAc structure.

OPN60 was subjected to mild acid hydrolysis to determine the monosaccharide composition of the glycans on the protein and thereby evaluate the structures observed in MS. The obtained monosaccharides were separated by high-pH anion exchange chromatography and subsequently monitored by pulsed electrochemical detection. The hydrolysates of OPN60 showed the presence of four types of monosaccharides GalNAc, GlcNAc, galactose and Sia (Table 3). The detected amounts of monosaccharides give approximately one mol of GalNAc/galactose and two moles of Sia per glycosylated threonine on OPN corresponding well with the glycans observed by MS.

The human OPN sequence contains two asparagines (Asn^{63} and Asn^{90}) in putative N-glycosylation motifs. MS analysis of peptides containing these residues showed that none of these asparagines are glycosylated in urinary OPN. In addition, incubation of urinary OPN with PNGase F did not result in altered migration when subjected to SDS-PAGE (data not shown). Furthermore, no trace of mannose was detected in the analysis of OPN monosaccharides (Table 3), substantiating the absence of N-linked glycosylations in human urinary OPN.

Discussion

The present work describes the purification and characterization of urinary OPN. Western blotting of urine obtained from seven healthy donors shows that urinary OPN exists in different forms migrating between 45 and 60 kDa (Fig. 1). In the OPN peak

eluting from the Vydac C_4 column three dominating forms were observed by Coomassie staining and immunoblotting (Fig. 3A). The strongly staining top band observed by Western blotting may consists of more than one isoform. This assumption is supported by Western blot detection of two bands in the samples containing OPN60 using the monoclonal antibodies 1H3 (faint) and 3D9 (Fig. 3B).

This study indicates that the N-terminal fragments OPN45 and OPN50 are generated from the full-length molecule by proteolytic cleavage at Arg^{228}-Leu^{229} and/or Tyr^{230}-Lys^{231} in urine. Though two bands are seen in SDS-PAGE, representing OPN45 and OPN50, only one broad peak is observed by MS suggesting that the mass difference between the fragmented OPNs is not large enough to give separation in linear MALDI-TOF-MS. No heterogeneity at the identified O-glycosylation sites was observed. However, differences in the glycans at the individual sites might account for the observed migration of OPN45 and OPN50 during SDS-PAGE.

OPN is present in human urine in different fragmented forms and it is therefore relevant to speculate on how these forms are generated. The protein has previously been shown to be a substrate for metalloproteinase (MMP)-3 and -7 [40] and thrombin [41]. In Figure 5 the cleavage sites of these proteolytic enzymes are compared to the observed fragmentation patterns of the characterized urinary OPN, showing that neither MMP-3, MMP-7 nor thrombin have been reported to cleave OPN at the sites reported in this study. It is not clear whether OPN45/OPN50 is the result of cleavage by specific proteases in the urinary secretory system. The cleavage sites identified in this study points in two directions. The cleavage of Arg^{228}-Leu^{229} could be catalysed by a thrombin-type of protease, whereas the cleavage site Tyr^{230}-Lys^{231} fits the specificity of a chymotrypsin-type of protease. However, it remains to be shown which proteases that are actually responsible for the cleavage of OPN in urine. Kidney cells have been reported to produce an OPN peptide that are thought to represent tissue-specific intracellular processing of the intact protein [42], which supports the hypothesis that OPN45 and OPN50 are proteolytically derived fragments of the intact protein. Alternative mRNA splicing could also be speculated to be responsible for the presence of the truncated OPN forms. However, the region containing the cleavage sites is encoded by exon 7 of the OPN gene and no intron-exon junction is located in the vicinity. It is therefore a much more plausible explanation that the N-terminal fragments are products of proteolytic activity rather than alternative mRNA splicing.

Interestingly, no C-terminal fragments corresponding to Leu^{229}/Lys^{231}-Asn^{298} were detected by the polyclonal antibody in the Western blot of urine (Fig. 1). This indicates that the C-terminal of urinary OPN is completely degraded when OPN45 and OPN50 are generated from OPN60. In support of this, no low molecular weight C-terminal OPN fragments were detected in Western blots of human urine using different monoclonal OPN antibodies with epitopes mapped to the C-terminal part of the protein [39]. OPN forms below the 40 kDa electrophoretic mobility range have been observed in urine from patients with kidney stones [24], whereas normal individuals had OPN forms migrating between 55- to 66-kDa as observed in this study. These low molecular weight forms of OPN were generated by serine proteases, and could reflect that augmented cleavage of urinary OPN could be a critical step in the formation of kidney stones.

OPN60 was shown to contain approximately eight phosphorylations and six phosphate groups were estimated to decorate OPN45/OPN50. This indicates that the region Leu^{229}/Lys^{231}-Asn^{298} missing in these cleaved forms contains about two phosphate groups. It is not clear whether some serines or threonines in OPN are phosphorylated to a higher degree than others. However, the fragment Leu^{229}/Lys^{231}-Asn^{298} that is missing in OPN45/OPN50 constitutes approximately one fourth of the amino acids in OPN. So, the observation that this fragment contains two out of eight phosphorylations suggests that the phosphate groups decorating the intact molecule are evenly distributed. The degree of phosphorylation on urinary OPN is significantly lower than the levels observed in milk OPN [27, 28], showing tissue-specific phosphorylation. A comparison of OPN from human milk and urine with regard to PTMs is shown in Figure 5. It is interesting to observe that of the 36 phosphorylation sites previously located in human milk OPN, 30 sites were also identified in human urinary OPN. However, the average phosphate content of the urinary isoform is only about one third of the milk isoform. In both urine and milk the highly anionic regions of OPN composed of multiple acidic amino acids and phosphorylations could constitute potential binding sites for minerals and calcium salts. These anionic regions could therefore enable OPN to form soluble complexes with calcium ions and thereby inhibit unintentional calcium precipitation and crystallization. Whether the different degrees of phosphorylation of human milk and urinary OPN are due to tissue-specific phosphorylation or dephosphorylation is not known.

Urinary OPN was shown to be sulphated at Tyr^{165}. This residue has recently been shown to be sulphated in rat bone OPN [29], and OPN produced from canine kidney cells has also been shown to be sulphated by metabolic labelling [42]. Tyr^{165} is conserved in mouse, rat and rabbit but not present in cow, sheep, pig and chicken indicating that sulphation of the protein is specie-dependent. No indication of a sulphate group on Tyr^{165} was observed in human milk OPN showing that this modification is also tissue-specific.

In this study, urinary OPN has been shown to contain five O-glycosylated threonines (Thr^{118}, Thr^{122}, Thr^{127}, Thr^{131}, and Thr^{136}). As shown in Figure 5, all O-linked glycans identified in human urine OPN are also present in human milk OPN. It appears that the glycans in urinary OPN predominantly consist of a disialylated GalNAc-galactose core. This glycan structure has also been described in OPN from rat bone and mouse fibroblasts and osteoblasts [29, 30]. No N-linked glycosylations were identified on urinary OPN at the two putative motifs (Asn^{63} and Asn^{90}). This is consistent with data on milk, bone and fibroblast OPN [27-30]. Normal rat kidney cells have been shown to produce both phosphorylated and non-phosphorylated forms of OPN *in vitro*, and the non-phosphorylated isoform contained N-linked carbohydrates [37], whether this is also the case *in vivo* remains to be shown.

In summary, human urine contains different forms of OPN representing the full-length protein and truncated forms lacking the C-terminal fragment Leu^{229}/Lys^{231}-Asn^{298}. The intact protein contains approximately eight phosphate groups distributed over 30 phosphorylation sites, whereas the fragments contain approximately six phosphate groups. In addition, one sulphate group and five O-glycosylated threonines were identified in urinary OPN. The PTMs of urinary OPN reported here are likely to play key roles in the protein's regulation of mineral crystallization in urine. Further studies are necessary to investigate if different PTMs could account for the pleiotropic role of OPN as both an inhibitor and promoter of renal stone formation.

References

1 Franzén, A. and Heinegård, D. (1985) Isolation and characterization of two sialoproteins present only in bone calcified matrix. Biochem. J. **232**, 715-724.

2 Sodek, J., Ganss, B. and McKee, M. D. (2000) Osteopontin. Crit. Rev. Oral Biol. Med. **11**, 279-303.

3 Ashkar, S., Weber, G. F., Panoutsakopoulou, V., Sanchirico, M. E., Jansson, M., Zawaideh, S., Rittling, S. R., Denhardt, D. T., Glimcher, M. J. and Cantor, H. (2000) Eta-1 (osteopontin): an early component of type-1 (cell-mediated) immunity. Science **287**, 860-864.

4 Rittling, S. R. and Chambers, A. F. (2004) Role of osteopontin in tumour progression. Br. J. Cancer **90**, 1877-1881.

5 Giachelli, C. M. and Steitz, S. (2000) Osteopontin: a versatile regulator of inflammation and biomineralization. Matrix. Biol. **19**, 615-622.

6 Chellaiah, M. A., Biswas, R. S., Rittling, S. R., Denhardt, D. T. and Hruska, K. A. (2003) Rho-dependent Rho kinase activation increases CD44 surface expression and bone resorption in osteoclasts. J. Biol. Chem. **278**, 29086-29097.

7 Hunter, G. K., Kyle, C. L. and Goldberg, H. A. (1994) Modulation of crystal formation by bone phosphoproteins: structural specificity of the osteopontin-mediated inhibition of hydroxyapatite formation. Biochem. J. **300**, 723-728.

8 Boskey, A. L., Maresca, M., Ullrich, W., Doty, S. B., Butler, W. T. and Prince, C. W. (1993) Osteopontin-hydroxyapatite interactions in vitro: inhibition of hydroxyapatite formation and growth in a gelatin-gel. Bone Miner. **22**, 147-159.

9 Shiraga, H., Min, W., VanDusen, W. J., Clayman, M. D., Miner, D., Terrell, C. H., Sherbotie, J. R., Foreman, J. W., Przysiecki, C., Neilson, E. G. and Hoyer, J. R. (1992) Inhibition of calcium oxalate crystal growth in vitro by uropontin: another member of the aspartic acid-rich protein superfamily. Proc. Natl. Acad. Sci. U. S. A. **89**, 426-430.

10 Min, W., Shiraga, H., Chalko, C., Goldfarb, S., Krishna, G. G. and Hoyer, J. R. (1998) Quantitative studies of human urinary excretion of uropontin. Kidney Int. **53**, 189-193.

11 Rittling, S. R. and Feng, F. (1998) Detection of mouse osteopontin by western blotting. Biochem. Biophys. Res. Commun. **250**, 287-292.

12 Wesson, J. A., Worcester, E. M., Wiessner, J. H., Mandel, N. S. and Kleinman, J. G. (1998) Control of calcium oxalate crystal structure and cell adherence by urinary macromolecules. Kidney Int. **53**, 952-957.

13 Asplin, J. R., Arsenault, D., Parks, J. H., Coe, F. L. and Hoyer, J. R. (1998) Contribution of human uropontin to inhibition of calcium oxalate crystallization. Kidney Int. **53**, 194-199.

14 Lieske, J. C., Leonard, R. and Toback, F. G. (1995) Adhesion of calcium oxalate monohydrate crystals to renal epithelial cells is inhibited by specific anions. Am. J. Physiol. **268**, 604-612.

15 Ryall, R. L., Chauvet, M. C. and Grover, P. K. (2005) Intracrystalline proteins and urolithiasis: a comparison of the protein content and ultrastructure of urinary calcium oxalate monohydrate and dihydrate crystals. BJU Int. **96**, 654-663.

16 Wesson, J. A., Johnson, R. J., Mazzali, M., Beshensky, A. M., Stietz, S., Giachelli, C., Liaw, L., Alpers, C. E., Couser, W. G., Kleinman, J. G. and Hughes, J. (2003) Osteopontin is a critical inhibitor of calcium oxalate crystal formation and retention in renal tubules. J. Am. Soc. Nephrol. **14**, 139-147.

17 Mo, L., Liaw, L., Evan, A. P., Sommer, A. J., Lieske, J. C. and Wu, X. R. (2007) Renal calcinosis and stone formation in mice lacking osteopontin, Tamm-Horsfall protein, or both. Am. J. Physiol. Renal Physiol. **293**, 1935-1943.

18 Yamate, T., Kohri, K., Umekawa, T., Amasaki, N., Isikawa, Y., Iguchi, M. and Kurita, T. (1996) The effect of osteopontin on the adhesion of calcium oxalate crystals to Madin-Darby canine kidney cells. Eur. Urol. **30**, 388-393.

19 Yasui, T., Fujita, K., Asai, K. and Kohri, K. (2002) Osteopontin regulates adhesion of calcium oxalate crystals to renal epithelial cells. Int. J. Urol. **9**, 100-108.

20 Yamate, T., Kohri, K., Umekawa, T., Konya, E., Ishikawa, Y., Iguchi, M. and Kurita, T. (1999) Interaction between osteopontin on madin darby canine kidney cell membrane and calcium oxalate crystal. Urol. Int. **62**, 81-86.

21 Kohri, K., Suzuki, Y., Yoshida, K., Yamamoto, K., Amasaki, N., Yamate, T., Umekawa, T., Iguchi, M., Sinohara, H. and Kurita, T. (1992) Molecular cloning and sequencing of cDNA encoding urinary stone protein, which is identical to osteopontin. Biochem. Biophys. Res. Commun. **184**, 859-864.

22 McKee, M. D., Nanci, A. and Khan, S. R. (1995) Ultrastructural immunodetection of osteopontin and osteocalcin as major matrix components of renal calculi. J. Bone Miner. Res. **10**, 1913-1929.

23 Yasui, T., Fujita, K., Hayashi, Y., Ueda, K., Kon, S., Maeda, M., Uede, T. and Kohri, K. (1999) Quantification of osteopontin in the urine of healthy and stone-forming men. Urol. Res. **27**, 225-230.

24 Bautista, D. S., Denstedt, J., Chambers, A. F. and Harris, J. F. (1996) Low-molecular-weight variants of osteopontin generated by serine proteinases in urine of patients with kidney stones. J. Cell. Biochem. **61**, 402-409.

25 Kleinman, J. G., Wesson, J. A. and Hughes, J. (2004) Osteopontin and calcium stone formation. Nephron. Physiol. **98**, 43-47.

26 Kazanecki, C. C., Uzwiak, D. J. and Denhardt, D. T. (2007) Control of osteopontin signaling and function by post-translational phosphorylation and protein folding. J. Cell. Biochem. **102**, 912-924.

27 Sørensen, E. S., Højrup, P. and Petersen, T. E. (1995) Posttranslational modifications of bovine osteopontin: identification of twenty-eight phosphorylation and three O-glycosylation sites. Protein Sci. **4**, 2040-2049.

28 Christensen, B., Nielsen, M. S., Haselmann, K. F., Petersen, T. E. and Sørensen, E. S. (2005) Post-translationally modified residues of native human osteopontin are located in clusters: identification of 36 phosphorylation and five O-glycosylation sites and their biological implications. Biochem. J. **390**, 285-292.

29 Keykhosravani, M., Doherty-Kirby, A., Zhang, C., Brewer, D., Goldberg, H. A., Hunter, G. K. and Lajoie, G. (2005) Comprehensive identification of post-translational modifications of rat bone osteopontin by mass spectrometry. Biochemistry **44**, 6990-7003.

30 Christensen, B., Kazanecki, C. C., Petersen, T. E., Rittling, S. R., Denhardt, D. T. and Sørensen, E. S. (2007) Cell Type-specific Post-translational Modifications of Mouse Osteopontin Are Associated with Different Adhesive Properties. J. Biol. Chem. **282**, 19463-19472.

31 Gericke, A., Qin, C., Spevak, L., Fujimoto, Y., Butler, W. T., Sørensen, E. S. and Boskey, A. L. (2005) Importance of phosphorylation for osteopontin regulation of biomineralization. Calcif. Tissue Int. **77**, 45-54.

32 Jono, S., Peinado, C. and Giachelli, C. M. (2000) Phosphorylation of osteopontin

is required for inhibition of vascular smooth muscle cell calcification. J. Biol. Chem. **275**, 20197-20203.

33 Addison, W. N., Azari, F., Sørensen, E. S., Kaartinen, M. T. and McKee, M. D. (2007) Pyrophosphate inhibits mineralization of osteoblast cultures by binding to mineral, up-regulating osteopontin, and inhibiting alkaline phosphatase activity. J. Biol. Chem. **282**, 15872-15883.

34 Pampena, D. A., Robertson, K. A., Litvinova, O., Lajoie, G., Goldberg, H. A. and Hunter, G. K. (2004) Inhibition of hydroxyapatite formation by osteopontin phosphopeptides. Biochem. J. **378**, 1083-1087.

35 Hoyer, J. R., Asplin, J. R. and Otvos, L. (2001) Phosphorylated osteopontin peptides suppress crystallization by inhibiting the growth of calcium oxalate crystals, Kidney Int. 60, 77-82.

36 Worcester, E. M., Kleinman, J. G. and Beshensky, A. M. (1995) Osteopontin production by cultured kidney cells. Ann. N. Y. Acad. Sci. **760**, 266-278.

37 Singh, K., DeVouge, M. W. and Mukherjee, B. B. (1990) Physiological properties and differential glycosylation of phosphorylated and nonphosphorylated forms of osteopontin secreted by normal rat kidney cells. J. Biol. Chem. **265**, 18696-18701.

38 Ye, B., Skates, S., Mok, S. C., Horick, N. K., Rosenberg, H. F., Vitonis, A., Edwards, D., Sluss, P., Han, W. K., Berkowitz, R. S. and Cramer, D. W. (2006) Proteomic-based discovery and characterization of glycosylated eosinophil-derived neurotoxin and COOH-terminal osteopontin fragments for ovarian cancer in urine. Clin. Cancer Res. **12**, 432-441.

39 Kazanecki, C. C., Kowalski, A. J., Ding, T., Rittling, S. R. and Denhardt, D. T. (2007) Characterization of anti-osteopontin monoclonal antibodies: Binding sensitivity to post-translational modifications. J. Cell. Biochem. **102**, 925-935.

40 Agnihotri, R., Crawford, H. C., Haro, H., Matrisian, L. M., Havrda, M. C. and Liaw, L. (2001) Osteopontin, a novel substrate for matrix metalloproteinase-3 (stromelysin-1) and matrix metalloproteinase-7 (matrilysin). J. Biol. Chem. **276**, 28261-28267.

41 Senger, D. R., Perruzzi, C. A., Papadopoulos, A. and Tenen, D. G. (1989) Purification of a human milk protein closely similar to tumor-secreted phosphoproteins and osteopontin. Biochim. Biophys. Acta. **996**, 43-48.

42 Ullrich, O., Mann, K., Haase, W. and Koch-Brandt, C. (1991) Biosynthesis and secretion of an osteopontin-related 20-kDa polypeptide in the Madin-Darby canine kidney cell line. J. Biol. Chem. **266**, 3518-3525.

Figure legends

Fig. 1. Western blot analysis of human urinary OPN. Urine obtained from seven healthy donors analysed on a 16% tris-tricine gel by SDS-PAGE and detected by a polyclonal OPN antibody. Lane 1. Molecular weight standards. Lane 2-8: Urine samples from seven individuals.

Fig. 2. RP-HPLC chromatography of human urine proteins eluted from DEAE material. Separation was performed on a Vydac C_4 column in 0.1% TFA and proteins were eluted with a gradient of 80% acetonitrile (dashed line) at a flow rate of 0.85 ml/min. Proteins were monitored at 226 nm (solid line). Peaks containing OPN and trypsin inhibitor (HI30) are indicated. The insert shows the separation of proteins in the OPN containing peak on a Vydac C_{18} column by stepwise increasing concentrations of 75% 2-propanol.

Fig. 3. Analysis of urinary OPN. Samples were separated on 16% tris-tricine gels by SDS-PAGE, and proteins visualized by Coomassie staining or Western blotting with a polyclonal antibody or the monoclonal antibodies 1H3 or 3D9. (A) Lane 1: Coomassie staining of the OPN containing peak (from Fig. 2). Lane 2: Western blot detection with a polyclonal OPN antibody of the OPN containing peak (from Fig. 2). Lane 3: Coomassie staining of the peak containing OPN45 and OPN50 (from insert Fig. 2). Lane 4: Coomassie staining of the peak containing OPN60 (from insert Fig. 2). (B) Western blot detection with the monoclonal antibody 1H3 of peaks containing OPN45/OPN50 (lane 1) and OPN60 (lane 2) (from insert in Fig.2). Western blot detection with the monoclonal antibody 3D9 of peaks containing OPN45/OPN50 (lane 3) and OPN60 (lane 4) (from insert in Fig.2).

Fig. 4. MALDI-TOF mass spectrometric analysis of native and dephosphorylated urinary OPN. (A) The average mass peaks at ~37.7 kDa (black trace) and 37.1 kDa (grey trace) represent OPN60 before and after treatment with ALP. (B) The average mass peaks at ~29.3 kDa (black trace) and 28.8 kDa (grey trace) represent the N-terminal OPN fragments before and after treatment with ALP.

Fig. 5. Posttranslational modifications in human urinary and milk OPN [28]. Phosphorylations (black), a sulphation (black) and glycosylations (grey) are highlighted. The glycan structures observed in urinary OPN are indicated; GalNAc (black squares), galactose (grey diamonds) and Sia (white circles). The cleavage sites observed in OPN45, OPN50 and OPN60 from urine are indicated by black arrows. Known proteolytic cleavage sites for MMP-3 and MMP-7 [40] and thrombin [41] are indicated by grey arrows.

Fig. 6. MALDI-TOF MS in linear mode of a sulphated peptide. (A) MS spectrum of a fraction containing the peptides Gln^{36}-Lys^{61} and Arg^{160}-Lys^{187}. The mass at *m/z* 3466.42 corresponds to the peptide Arg^{160}-Lys^{187} modified by three phosphate/sulphate groups. (B) MS after treatment with alkaline phosphatase (ALP). The mass at *m/z* 3306.43 corresponds to Arg^{160}-Lys^{187} with an excess mass of ~80 Da indicating the presence of a sulphate group. (C) MS after treatment with alkaline phosphatase and subsequently arylsulphatase. The mass loss of 80 Da from Arg^{160}-Lys^{187} upon treatment with the sulphatase shows that this peptide contained two phosphorylations and one sulphate group.

Table 1: Thrombin cleavage of OPN45/OPN50

The fragments were identified by N-terminal sequence and MALDI-TOF-MS analyses. The observed molecular masses were determined by MALDI-TOF-MS in linear mode. Mass difference is that between the observed and calculated average masses. The type of modification corresponding to the mass difference is given in parentheses: phosphorylation (P), sulphation (S) and oxidation of methionine (Mox).

Fragment	Observed mass (Da)	Calculated mass (Da)	Mass difference (Da)
Ile^{1}-Arg^{152}	20600	16890.5	3709.5 (P and *O*-glycans)
Val^{3}-Arg^{152}	20600	16680.2	3919.8 (P and *O*-glycans)
Ser^{153}-Arg^{228}	8820.9/8740.5/8658.9	8642.2	178.7/98.3/16.7 (P and/or S, Mox)
Ser^{153}-Tyr^{230}	9173.6/9093.6/9013.5	8918.5	255.1/175.1/95.0 (P and/or S, Mox)

Table 2: Characterization of phosphorylated peptides

The peptides from the tryptic and thermolytic (Gln^{36}/Ser^{62}-Arg^{143}) digests of OPN were characterized by MALDI-TOF-MS. The number of phosphates indicates the different phosphorylation variants of each individual peptide observed by MS. MGCK, mammary gland casein kinase, CKII, casein kinase II.

Peptide	Ser/Thr in MGCK or CKII motif	No. phosphates
Gln^{5}-Lys^{19}	Ser^{8}, Ser^{10}, Ser^{11}	3/2
Gln^{5}-Lys^{35}	Ser^{8}, Ser^{10}, Ser^{11}	3
Gln^{15}-Lys^{35}		0
Tyr^{20}-Lys^{35}		0
Gln^{36}-Lys^{54}	Ser^{46}, Ser^{47}, Thr^{50}	2/1/0
Gln^{36}-Lys^{61}	Ser^{46}, Ser^{47}, Thr^{50}, Thr^{57}, Ser^{60}	2/1/0
Gln^{55}-Lys^{61}	Thr^{57}, Ser^{60}	0
Thr^{57}-His^{68}	Thr^{57}, Ser^{60}, Ser^{62}, Ser^{65}	2/1
Ser^{62}-His^{68}	Ser^{62}, Ser^{65}	0
Met^{69}-His^{80}		0
Met^{72}-His^{80}		0
Val^{81}-Ser^{86}	Ser^{83}, Ser^{86}	1/0
Ile^{87}-Asp^{94}	Ser^{89}, Ser^{92}	1/0
Ile^{87}-Glu^{115}	Ser^{89}, Ser^{92}, Thr^{98}, Ser^{101}, Ser^{104}, Ser^{107}, Ser^{110}, Ser^{113}	6/5/4/3
Val^{95}-Ser^{107}	Thr^{98}, Ser^{101}, Ser^{104}, Ser^{107}	2/1/0
Val^{95}-Glu^{115}	Thr^{98}, Ser^{101}, Ser^{104}, Ser^{107}, Ser^{110}, Ser^{113}	5/4/3/2/1
Thr^{98}-Glu^{115}	Thr^{98}, Ser^{101}, Ser^{104}, Ser^{107}, Ser^{110}, Ser^{113}	5/4/3
Ser^{101}-Glu^{115}	Ser^{101}, Ser^{104}, Ser^{107}, Ser^{110}, Ser^{113}	4/3/2
Ser^{104}-Glu^{115}	Ser^{104}, Ser^{107}, Ser^{110}, Ser^{113}	2/1
His^{108}-Glu^{115}	Ser^{110}, Ser^{113}	2/1/0
Ser^{110}-Glu^{115}	Ser^{110}, Ser^{113}	1/0
Gly^{144}-Arg^{152}		0
Phe^{158}-Lys^{187}	Thr^{169}, Ser^{175}, Ser^{179}	2/1/0 (± 1 sulphation)
Arg^{160}-Lys^{187}	Thr^{169}, Ser^{175}, Ser^{179}	2/1/0 (± 1 sulphation)
Ala^{188}-Arg^{204}	Ser^{199}	1/0
Gly^{205}-Lys^{225}	Ser^{208}, Ser^{212}, Ser^{218}	3/2/1/0
Leu^{229}-Arg^{232}		0
Lys^{233}-Arg^{255}	Ser^{238}, Ser^{247}, Ser^{251}, Ser^{254}	4/3/2/1
Glu^{256}-Lys^{274}	Ser^{259}, Ser^{264}	2/1/0
Ser^{275}-Lys^{283}	Ser^{275}	1/0
Phe^{284}-Asn^{298}	Ser^{287}, Ser^{292}, Ser^{294}	3/2/1
Ile^{286}-Asn^{298}	Ser^{287}, Ser^{292}, Ser^{294}	2/1/0

Table 3: Characterization of glycosylations on urinary OPN

The peptides were characterized by Edman sequencing and MALDI-TOF-MS. Glycosylated residues are indicated with bold letters.The observed molecular masses were determined by MALDI-TOF-MS in linear mode. Mass difference is that between the observed and calculated average masses. Based on the MS data, the composition of the individual glycans is suggested in parentheses: GalNAc, N-acetylgalactosamine; GlcNAc, N-acetylglucosamine; Sia, sialic acid. The carbohydrate composition of purified OPN was determined as described in Experimental. n.d.: not detected.

Molecular masses of glycopeptides determined by MS

Peptide	Observed mass (Da)	Calculated mass (Da)	Mass difference (Da)
L^{116}V**T**DFP**T**DLPA**T**E^{128}	(major) 4261.24	1419.56	2841.68 ($GalNAc_3$, $Galactose_3$, Sia_6)
	(major) 3970.97	1419.56	2551.41 ($GalNAc_3$, $Galactose_3$, Sia_5)
	(minor) 3679.83	1419.56	2260.27 ($GalNAc_3$, $Galactose_3$, Sia_4)
V^{129}F**T**PVVP**T**VDT^{139}	(minor) 3562.97	1175.36	2387.61 ($GalNAc_2$, GlcNAc, $Galactose_2$, Sia_5)
	(major) 3069.50	1175.36	1894.14 ($GalNAc_2$, $Galactose_2$, Sia_4)
	(minor) 2778.22	1175.36	1602.86 ($GalNAc_2$, $Galactose_2$, Sia_3)

Carbohydrate composition (mol monosaccharide/mol OPN)

GalNAc: 5.15	GlcNAc: 1.34	Galactose: 4.95	Sialic Acid: 11.18	Fucose: n.d.	Mannose: n.d.

Biochemical Journal Immediate Publication. Published on 12 Dec 2007 as manuscript BJ20071021

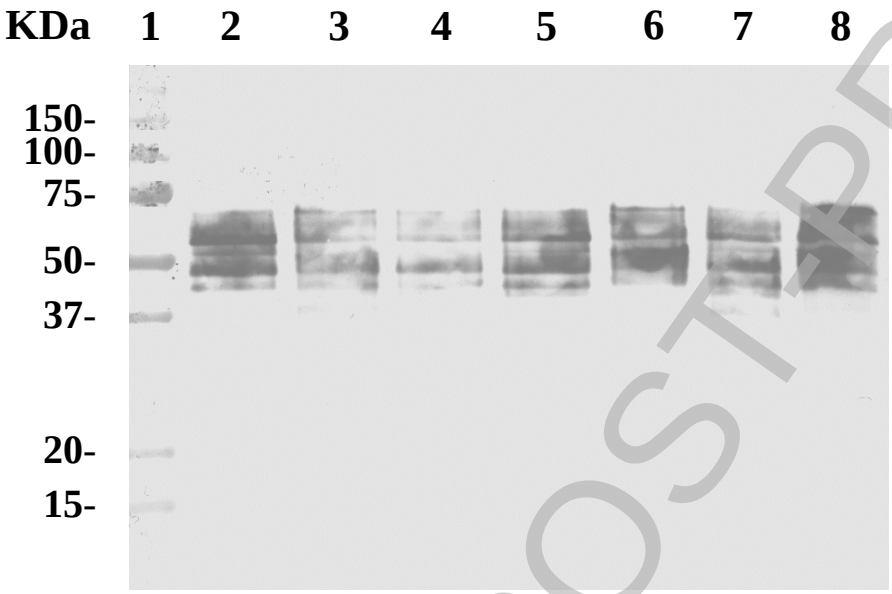

Figure 1

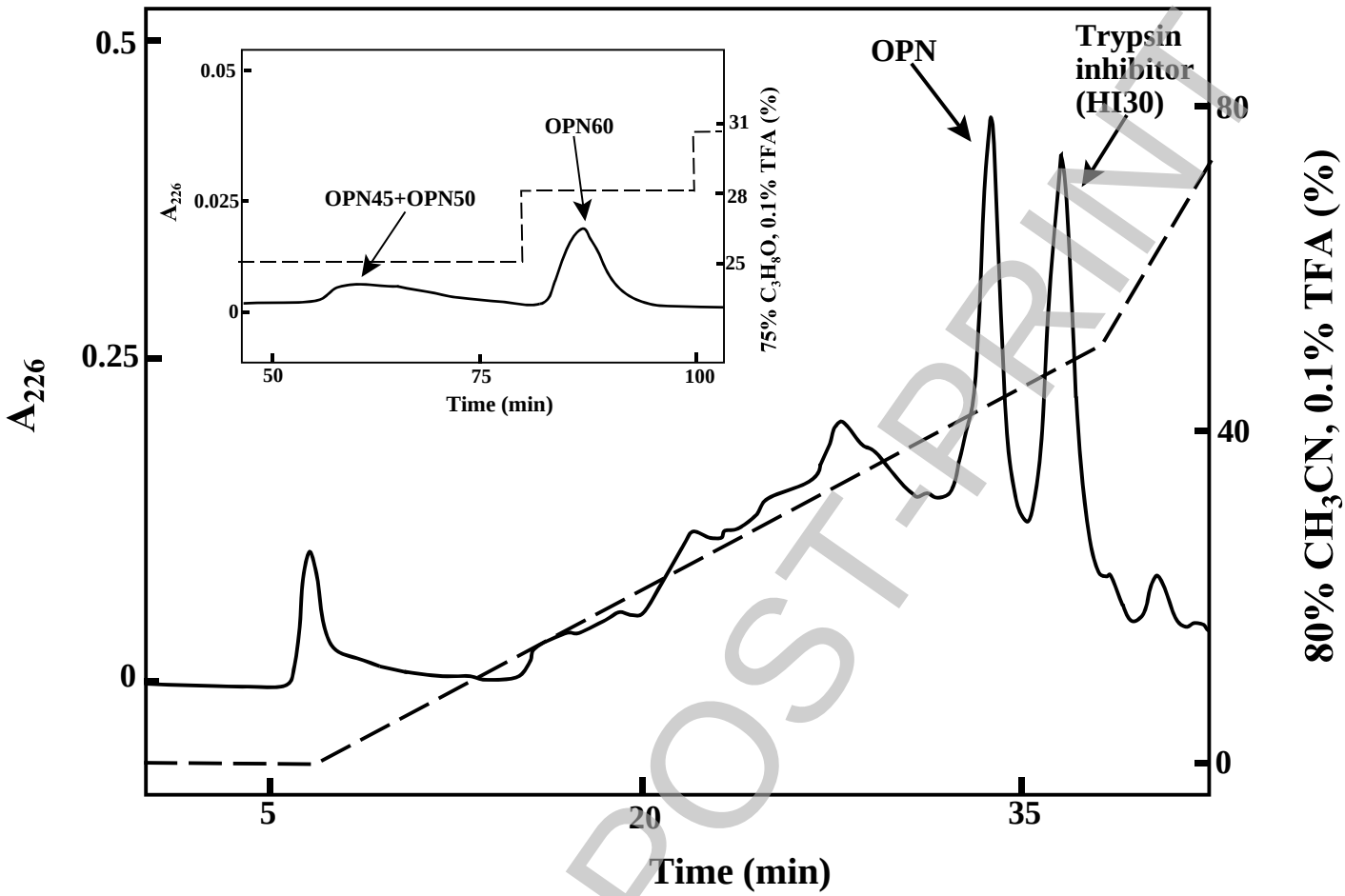

Figure 2

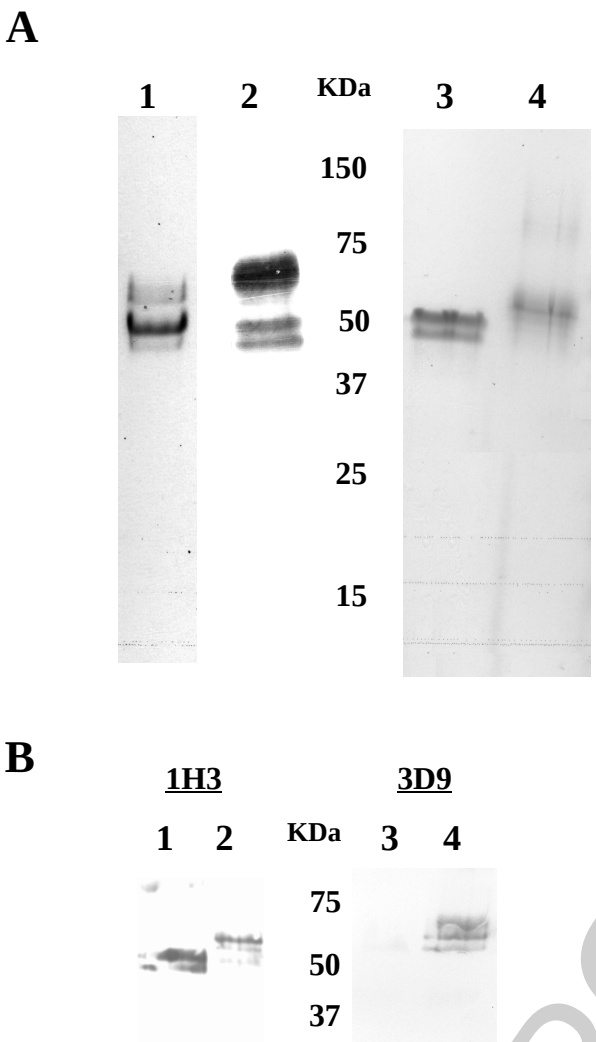

Figure 3

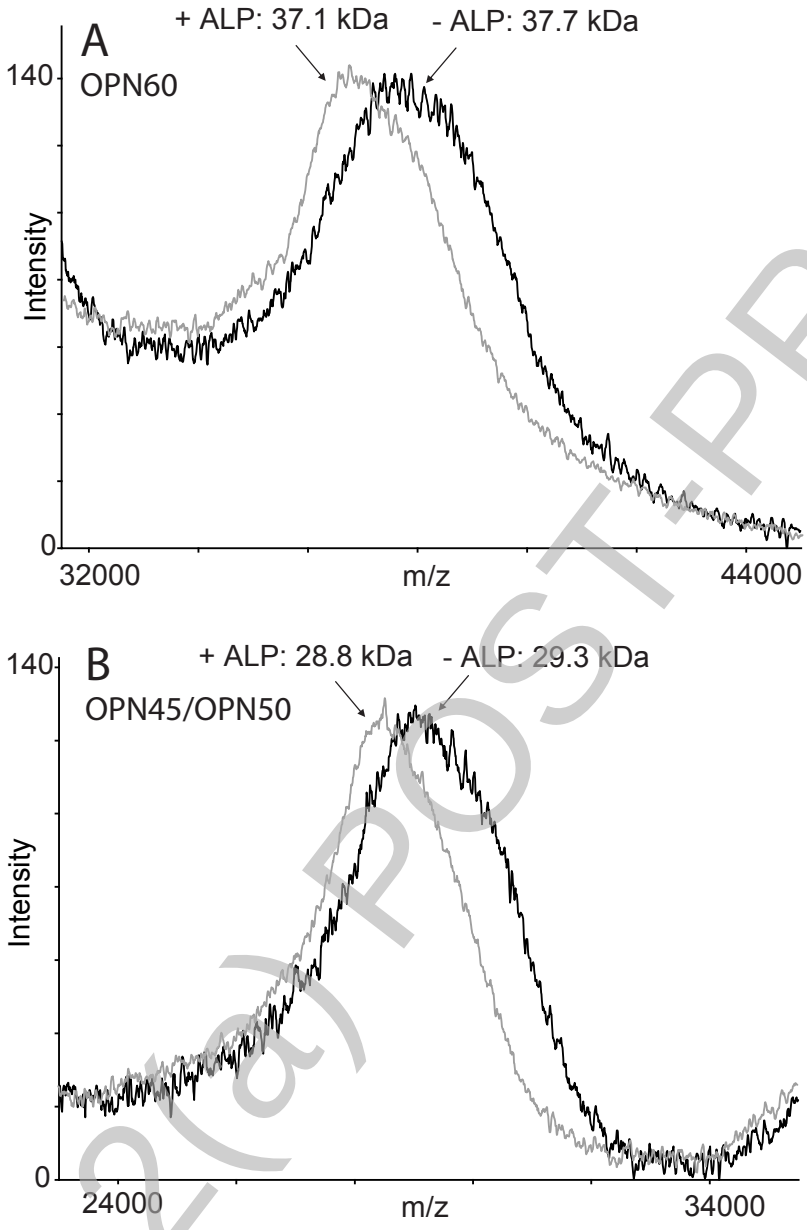

Figure 4

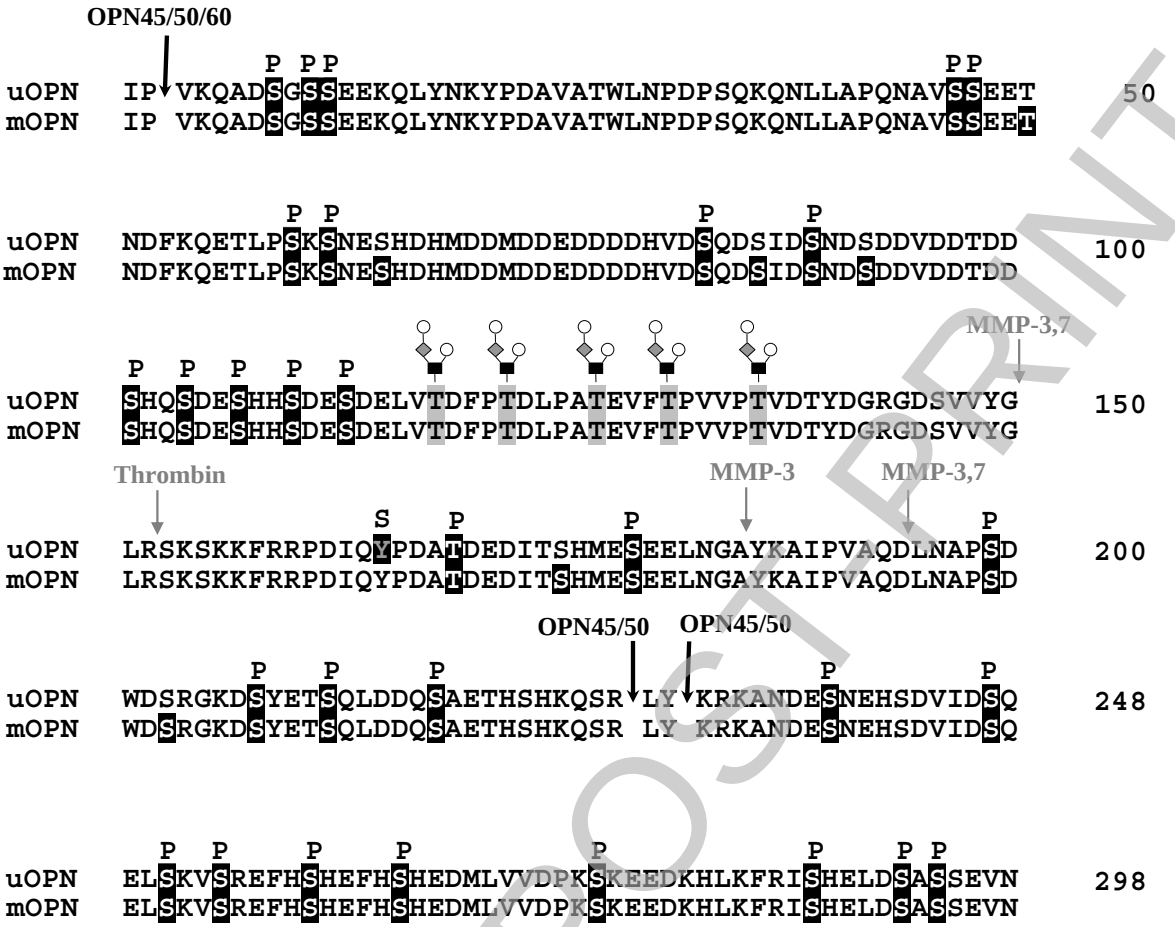

Figure 5

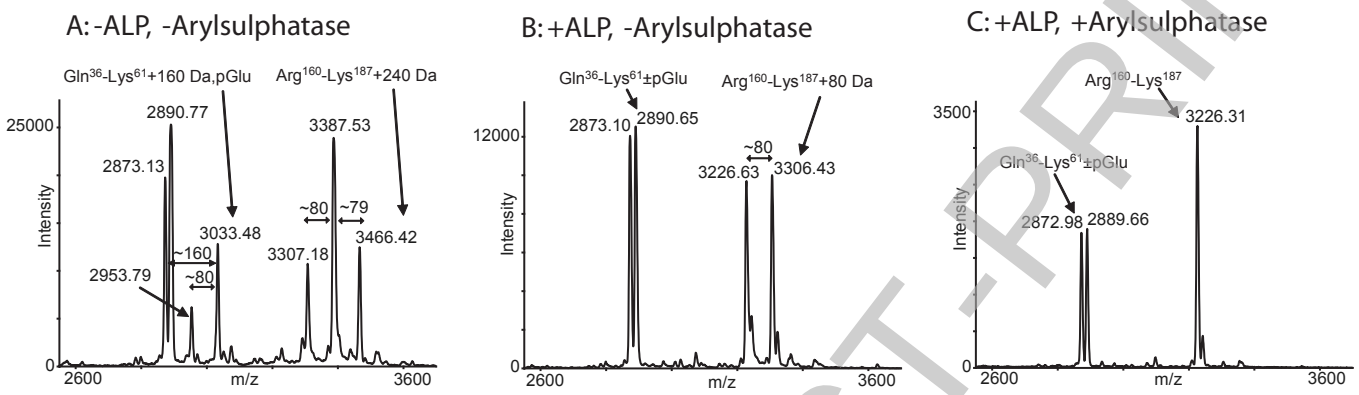

Figure 6